ABSTRACT

MODELING AND EXPERIMENTAL EVALUATION OF HAPTIC RENDERING IN TOUCH SURFACES USING MULTIFREQUENCY ELECTROSTATIC ACTUATION

by Santosh Mohan Rajkumar

Available devices with smaller touchscreen displays (TSDs) offer users adequate haptic feedback, whereas larger TSDs still lack meaningful tactile sensations. This study is focused on rendering vibrotactile feedback on large TSDs. Existing methods for localized vibrotactile rendering on large TSDs use many actuators. Practically, using many actuators is not desirable due to space constraints, power supply limitations, etc., for consumer-centric large TSD devices. Therefore, this study investigates localized vibrotactile feedback on large TSDs using a restricted number of electrostatic resonant actuators (ERAs). Using flexible boundary conditions combined with multi-frequency excitation, a novel method is presented to render localized vibrotactile feedback for two types of large TSDs: a narrow touch bar and a rectangular touch surface. A method for managing/positioning localized haptic feedback on large TSDs is also investigated. In-house finite-element-based simulation models of TSDs are developed along with experimental prototypes for verifying the vibrotactile performance. The modeling and analysis strategy presented here is general and can be extended for haptic rendering methods of different touch surfaces, actuators, and boundary conditions. Finally, model-based parametric studies are presented for better design considerations and improved vibrotactile intensity.

MODELING AND EXPERIMENTAL EVALUATION OF HAPTIC RENDERING IN TOUCH SURFACES USING MULTIFREQUENCY ELECTROSTATIC ACTUATION

A Thesis

Submitted to the

Faculty of Miami University

in partial fulfillment of

the requirements for the degree of

Master of Science

by

Santosh Mohan Rajkumar

Miami University

Oxford, Ohio

2023

Advisor: Dr. Kumar V. Singh

Advisor: Dr. Jeong-Hoi Koo

Reader: Dr. James R. Chagdes

This Thesis titled

MODELING AND EXPERIMENTAL EVALUATION OF HAPTIC RENDERING IN TOUCH SURFACES USING MULTIFREQUENCY ELECTROSTATIC ACTUATION

by

Santosh Mohan Rajkumar

has been approved for publication by

The College of Engineering and Computing

and

Department of Mechanical and Manufacturing Engineering

_____

Dr. Kumar V. Singh

_____

Dr. Jeong-Hoi Koo

_____

Dr. James R. Chagdes

Table of Contents

List of Tables

List of Figures

Dedication

মোৰ পিতৃ-মাতৃ আৰু সমাজৰ প্ৰতি উৎসৰ্গা কৰিলোঁ।

Translation: *Dedicated to my family and community.*

Acknowledgments

First and foremost, I would like to express my heartfelt gratitude to my supervisor, Prof. Kumar Vikram Singh, for his unwavering support and guidance throughout my MS journey. It is the trust in him that motivated me to embark on a transatlantic journey of 9000 miles to pursue my graduate studies at Miami University. Simultaneously, I would also like to extend my appreciation to my co-advisor, Prof. Jeong-Hoi Koo, whose guidance has played a pivotal role in shaping this research. Their invaluable mentorship, expertise, encouragement, and camaraderie have greatly contributed to this endeavor. I consider myself truly fortunate to have had the privilege of working under their guidance. I am grateful for the opportunity to meet with them every week, discuss progress, and receive valuable feedback and suggestions. I am grateful for your continuous efforts in exposing me to intriguing challenges and consistently seeking out opportunities for your students.

I would like to thank Dr. Tae-Heon Yang for all the support and troubleshooting on the hardware side of this research. Also, thank you for making me learn how to make expressive scientific graphics.

I would also like to thank Dr. James R. Chagdes for your valuable comments and suggestions for improvements in this research.

Thanks to my undergraduate supervisor Dr. Rajeeb Dey, for always providing guidance and support. Thank you for suggesting the ME MS program at Miami University.

Thank you, all my friends in Oxford and colleagues at Miami University. Without you people, this journey would not have been interesting and enjoyable.

I sincerely thank the MME Department and Miami University for a nurturing and stimulating environment, fostering a passion for research, and full financial support during my MS program.

Finally, a very special thanks to my parents for believing in me and never doubting my decision to leave a Fortune 150 job and pursue higher education 9000 miles west, and the taken-for-granted love, affection, and support.

Declaration

This thesis is the result of my own work and collaborations in which I was always the scientific lead. This dissertation has not been previously submitted, in part or whole, to any university or institution for any degree, diploma, or other qualification. The ideas herein have appeared/will appear in the following published papers as of June 2023:

1. Rajkumar, S.M., Singh, K.V. and Koo, J.H., "Modeling and Analysis of a Thin Plate with Multiple Harmonic Excitations for Vibrotactile Touch Display Applications," in *International Design Engineering Technical Conferences and Computers and Information in Engineering Conference*. American Society of Mechanical Engineers, 2023 (Accepted for publication).

2. Rajkumar, S.M., Singh, K.V., Yang, T.H. and Koo, J.H., "Modeling and Experimental Evaluation of Haptic Localization Using Electrostatic Vibration Actuators," in *IEEE Access*, vol. 11, pp. 18582-18589, 2023.

3. Rajkumar, S.M., Singh, K.V. and Koo, J.H., "October. Modeling and analysis of multiple electrostatic actuators on the response of vibrotactile haptic device," in *ASME International Mechanical Engineering Congress and Exposition* (Vol. 86625, p. V001T01A004). American Society of Mechanical Engineers,2022.

Vita

1995	Born in Sibsagar, Assam, India
(Aug 2013 – May 2017)	Bachelor of Technology (B.Tech.) in Electrical Engineering, **National Institute of Technology Silchar**, India
(Jun 2017 – Dec 2020)	Senior Engineer, **Indian Oil Corporation Limited** (A Fortune 150 Corporation), Dimapur, India
(Jan 2021 – Jun 2023)	Master of Science in Mechanical Engineering, **Miami University**
(Jan 2021 – May 2023)	Graduate Teaching Assistant, **Miami University**

1. Introduction

This chapter addresses the motivations and significance behind conducting this study. The importance of localized haptic feedback in large touch screen displays (TSDs) is highlighted. The main objectives of the study are outlined in this chapter, along with the suggested approach crucial to accomplishing these overall objectives. Further, the outline of this thesis is delineated.

1.1. Motivations and Significance

Large high-resolution displays convey rich information to the user [1]. Large size displays also provide a greater field of view, enabling faster completion of cognitively loaded tasks for a user [2]. Also, the ability to use multiple windows in large displays enhances the user's productivity[2]. Apart from personal computing devices/gadgets, large touch screen displays (TSDs) are used in modern automotive center consoles *or In-vehicle Information Systems* (IVISs), which typically include a variety of functionalities such as media playback, navigation guidance system, climate control system, and vehicle performance system [3]. Automotive TSDs are approaching a size of 15 inches or more and sometimes edge to edge of the vehicle [4]. Furthermore, the most essential way of controlling Digital musical instruments (DMIs) is touch-based interaction [5]. The touch-based interaction in DMIs commonly done using large touch screens. Different DMIs as applications are also available for tablet devices and touch-based laptop computers (e.g., applications available for Apple iPad such as GarageBand, Simply Piano, and Zenbeats). A potential application of DMIs with large interactive TSDs is in Neurological Music Therapy (NMT) for supporting the sensorimotor regulation of individuals with autism [6]. Large TSDs are also used as kiosks in a multitude of applications [7]. Such kiosks are used by the public to obtain information and service in places like airports, hotels, museums, and hospitals. TSD-based Kiosks are also used for point-of-sale/point-of-service purposes in retail stores, shopping malls, and restaurants, as depicted in Figure 1Figure 1(a). Vending machines and ATMs also use large TSDs to offer public service. Figure 1(b) shows a vending machine using a large TSD for user inputs. Another use of large TSDs is in interactive education and training. Tablet devices are being increasingly used by children to learn emergent literacy skills such as alphabets, words, sounds, reading, and writing [8],[9]. Tabletop setups using large TSDs are also found in use for collaborative learning [10], [11]. In medical training, like collaborative patient diagnosis and treatment, large tabletop TSDs can be used [12]. Moreover, large TSDs also find applications in the medical field, such as various medical device control & information system, ambulance operator information systems, etc. [13]. With touchscreens, medical professionals can access all information easily. In modern flight decks, TSDs have been introduced, as demonstrated in the Boeing 777-X shown in Figure 2, to improve the interaction between humans and aircraft [14]. Additionally, modern-day virtual reality (VR) applications require large TSDs for users to have an immersive experience. A larger screen size provides better immersion for the user [15], [16]. Some of the virtual reality applications include immersive gaming, industrial planning, and robotic teleoperation [17], [18].

Haptic feedback in TSDs enhances user interaction, increases user input speed, and makes the user experience immersive [19]. Tactile rendering on TSD involves creating and replicating physical sensations that can be felt through touch [20]. Tactile rendering conveys abundant, instinctive, and authentic information without requiring a high level of intricacy and expense. Out

of the different types of tactile displays available, those that generate vibrations (vibrotactile rendering) are more commonly used and have a greater comprehension level thanethods that manipulate other tactile sensations, such as constant pressure, skin extension, or friction [20].

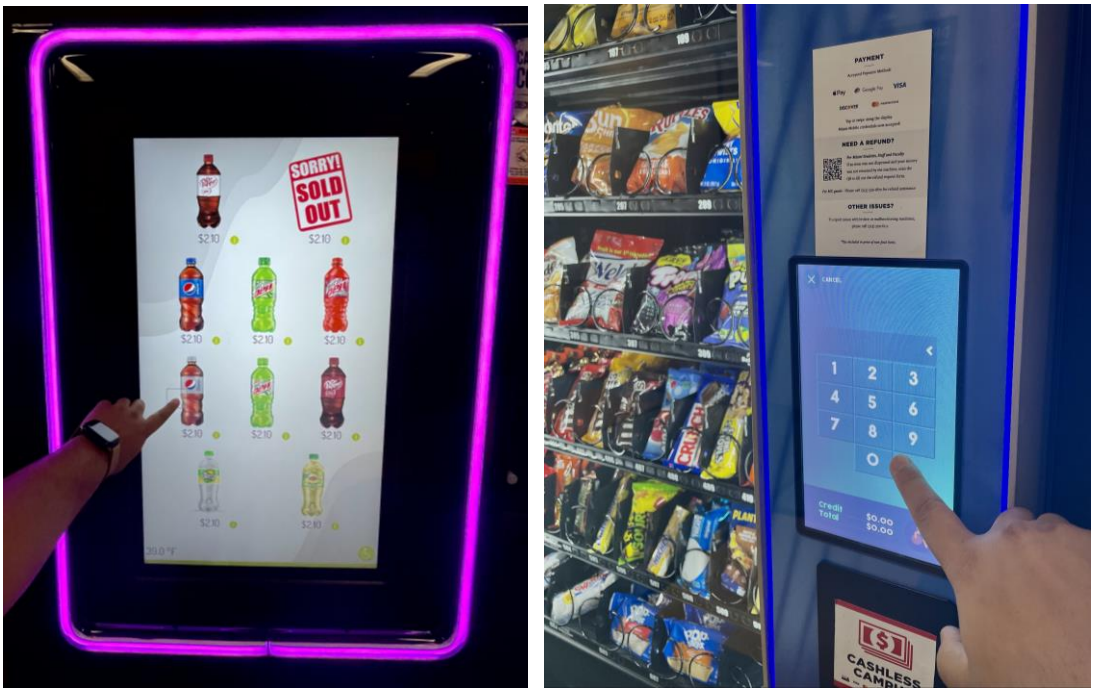

(a) (b)

Figure 1: (a) TSD-based kiosk for point-of-sale purposes (b) Vending machine using large TSD for user input.

Figure 2: Large TSDs used in deck of the Boeing 777-x [21]

Large TSDs in the market face a considerable problem as they either lack localized haptic feedback or provide insufficient feedbackompared to the smaller TSDs found in mobile devices [22]. The absence or inadequate haptic feedback in larger TSDs can have a detrimental effect on the user experience, leading to reduced functionality and accuracy in input [19]. In the context of automotive center consoles, the absence of haptic feedback in large TSDs creates a sense of unfamiliarity for drivers due to the absence of familiar physical buttons and can contribute to driver distraction which can lead to accidents [4]. Similarly, in digital musical instruments that utilize sizable touch surfaces, haptic feedback becomes crucial for enhancing performance and enabling the instrument to be accessible to performers with hearing or visual impairments [23]. Large TSDs used in medical devices sometimes need to be operated in rainy environments or with water. Also, vibrations due to road conditions may affect the accuracy of input for ambulance operator information systems [13]. Haptic feedback in large TSDs can improve the accuracy of inputs for medical workers and ambulance staff in such conditions. In the case of TSDs used in flight decks, turbulence or vibrations occurring during flights can potentially increase the chance of mistakes and slower response time for the pilot [24]. Moreover, touch-based kiosks in public places, which are generally crowded and noisy, can make user interaction convenient by incorporating localized haptic feedback. Further, with the advancement of graphics processors, high-definition games are available for tablet pcs or small computers. The presence of localized haptic feedback in large TSDs used for gaming can provide users with an immersive experience with a better degree of control. For VR applications, the presence of haptic feedback makes the user experience immersive and effective. Therefore, haptic feedback is essential in various applications of large TSDs, where localized rendering is required for an effective, realistic, and immersive user experience.

As discussed, adequate haptic feedback in devices with small TSDs, like mobile phones, is commercially available. But commercially available large TSDs still lack adequate haptic feedback. Hence, the motivation of this research is based on the need for haptic feedback generation in large touch screen displays (TSDs). Vibrotactile actuation is selected for rendering haptic feedback on large TSDs for simplicity and economical design. This work aims to generate localized vibrotactile feedback on large TSDs. Managing the localized vibrotactile feedback on large TSDs is also a concern of this study so that multi-touch and multi-zone haptics is possible. The inclusion of vibrotactile feedback in devices with large TSDs will not only enhance user experience and immersion but also make large TSDs germane to critical applications like medical, aviation, automotive, etc.

The lack of adequate vibrotactile feedback in devices with large TSDs can be attributed to the availability of a very small number of actuators capable of rendering tactile feedback of sufficient intensities. For large TSD applications, compact actuators such as piezo actuators and electrostatic vibration actuators are viable options [25]. The high power requirements limit Piezo actuators, and electrostatic vibration actuators are limited in vibration intensity due to the snap-in phenomenon. Using a dual-electrode configuration, a new electrostatic vibration actuator call an electrostatic resonating actuator (ERA) has been proposed [19]. The ERA overcomes the drawbacks due to the snap-in phenomenon and provides vibrations of significant intensities for large TSD applications [25]. Therefore, this study uses the ERA for haptic rendering on large TSDs.

Localized vibrotactile rendering on large TSDs using a suitable type of actuator is still challenging with rigid boundaries (e.g., fixed and pinned). For localized vibrotactile rendering, a

flexible connection is required at the boundaries of the TSDs [20]. With rigid boundaries, the TSD undergoing vibrotactile actuation ofteexhibits dead zones or nodes with little to no haptic feedback [26]. Existing localized vibrotactile methods for large TSDs mostly use rigid boundaries. Therefore, numerous actuators are used to excite the large TSDs so that dead zones or nodes can be eliminated and localized vibrotactile feedback can be rendered. The use of many actuators is often not practical for commercial purposes due to constraints like size or form factor and power supply limits. The contributions of this study are rooted in its novel basis of using a restricted number of actuators to render localized vibrotactile feedback on large TSDs with flexible boundaries.

Developing methods for localized vibrotactile feedback of desirable intensities on large TSDs, while considering factors like the choice of actuators and the number of them to be used, boundary conditions, type of excitations, and actuator placement, is challenging to accomplish through physical construction alone. Constructing multiple variations of such devices is impractical. To overcome this limitation, it is essential to develop generalizable simulation models for large TSDs. These models can be used to investigate and optimize the design of the TSD system, enabling the exploration of localized vibrotactile feedback. Additionally, these models can facilitate the extension of haptic rendering techniques to different materials and actuators, as well as control of the rendered localized haptic feedback. Therefore, this study tries to develop in-house mathematical simulation models of large TSDs with flexible boundaries and ERAs. Such simulation models can be easily developed in CAD design software like COMSOL, Solidworks, etc. However, there are some advantages of constructing in-house mathematical models compared to modeling in conventional CAD software such as increased adaptability and choices for customization. In addition, in-house models allow for implementing tailored and efficient solving algorithms for dynamic simulation. Further, the potential integration of in-house models with data analytics software, AI/ML libraries, and other programming interfaces enables convenient data manipulation, optimization, statistical analysis, and simulation.

As already stated, this research aims at generating and managing localized vibrotactile feedback on large TSDs using a restricted number of electrostatic vibration actuators. Eliminating dead zones of vibrations or nodes on a TSD under vibrotactile actuation with a limited number of actuators is facilitated using flexible boundary conditions. For developing methods for delivering and controlling localized haptic rendering, in-house simulation model-based studies are carried out. The significance of this work is as follows.

- The ability to render localized vibrotactile feedback on large TSDs with a restricted number of actuators allows for incorporating haptic feedback in devices and applications limited by compact size and low power consumption requirements.
- A generalizable model-based study for localized vibrotactile rendering on large TSDs enables a convenient extension of a rendering method to different types of touch surfaces, actuators, and boundaries.
- Management of localized haptic rendering on large TSDs provides the user with an immersive experience and paves the way for multi-touch and multi-zone haptics.

1.2. Objectives

The overarching goal of this study is to generate and manage localized vibrotactile feedback on large touchscreen displays (TSDs) using a limited number of electrostatic vibration actuators called electrostatic resonating actuators (ERAs). To achieve this goal, the following are the objectives of this research.

- **Prototype development:** Design and fabricate initial prototypes of large TSDs using ERAs with flexible boundary conditions. Provide the flexibility to independently control the excitation parameters, like amplitude, frequency, etc., of each ERA.
- **Mathematical modeling, simulation, and verification:** Based on the prototypes, develop in-house mathematical models for obtaining vibrotactile intensities at different spatial locations of the TSDs. The model should cater to multi-frequency excitations as the ERAs can be controlled independently. Validate the accuracy of mathematical models by comparing them with commercial software. Finally, verify the predictions from mathematical models using experimental data.
- **Method for localized vibrotactile rendering:** Develop a localization rendering strategy using a simulation model to achieve desirable vibrotactile feedback throughout the TSDs and verify this strategy experimentally.
- **Management of the localized vibrotactile rendering:** Come up with ways to manage or position the rendered vibrotactile feedback on desired locations of the TSDs.
- **Design considerations:** Using the mathematical models, present a statistical study that can aid in designing large TSDs with haptic feedback (for example, the number of actuators to be used, their placement, mechanical properties at the boundaries, etc.).

1.3. Approach

To accomplish the objectives listed above, the following steps are followed:

- **Fabrication of large TSD systems with ERAs:** To facilitate the manipulation of haptic rendered zones and dead zones of vibration or node points on large TSDs, two experimental prototypes are fabricated with flexible boundary conditions: a narrow bar-type touch surface and a rectangular touch surface**.** The bar-type touch surface is fabricated using an aluminum bar with two ERAs connected directly to the touch surface. The direct connection between the actuators and the touch surface gives rise to spring-damper boundary conditions. On the other hand, the setup for the rectangular touch surface is fabricated using an aluminum plate with two ERAs connected directly to the touch surface. In addition to the ERAs, the surface is also supported at the four corners with radial springs, referred to as boundary supports hereafter. The boundary supports, and direct connection of the ERAs give rise to spring-damper boundary conditions. The mechanical properties of the ERAs and the boundary supports are determined experimentally.
- **Mathematical model development:** To understand patterns of haptic rendering with different excitations of the ERAs, mathematical models of the bar type and the rectangular touch surface are developed, incorporating flexible boundaries. Finite-element method is used to mathematically develop models of both touch surfaces with the ERAs, and in-house codes for those models are developed in MATLAB. Care is taken while developing the codes so

that the models can be extended to different touch surface properties, the number of actuators, different boundaries, and different placement of the actuators.

- **Mathematical model verification & simulation:** Preliminary validation of the mathematical models developed is done by comparing the mode shapes computed using the in-house code with those computed in COMSOL, and by comparing the eigen frequencies with analytically derived standard rigid boundaries. There is a need to incorporate multi-frequency inputs for the simulation of the developed models, as the excitations of the ERAs can be controlled independently. The finite-element models of the touch surfaces involve sizeable systems of linear equations. Deriving a computationally efficient solution strategy for those models to obtain vibrotactile intensity at different spatial positions is crucial. This is because not only does a computationally efficient solution strategy save man-hours, it also makes parametric studies of responses, optimization, and other types of data analysis feasible. An analytical solution method is presented for the developed finite-element models of the touch surfaces. The mathematical models are verified by comparing their vibrotactile response with the response from the prototypes for similar excitations.
- **Localized haptic rendering:** To explore the localized haptic feedback rendering, the vibrotactile intensities of the finite-element models are to be analyzed for different actuator excitations and actuator configurations. Based on this analysis, we propose a localized haptic rendering method and verify it experimentally.
- **Management of localized haptic rendering:** Once the method(s) for localized haptic rendering is established, further study is carried out for managing or positioning localized vibrotactile feedback using a model-based study.
- **Design analysis and parametric study:** Statistical visualization and analysis of rendered vibrotactile feedback computed using the mathematical models of the touch surfaces are used to analyze the suitable placement of the ERAs, the number of them to be used, mechanical properties of the actuators and boundary supports for rich vibrotactile feedback. A parametric study is carried out to suggest a better design of TSDs for rich vibrotactile feedback.

1.4. Outline

This research study is presented in multiple chapters as follows.

- **Chapter 2:** This chapter introduces touch screen displays (TSDs) and their advantages and explores different haptic actuation methods available for TSDs, focusing on vibrotactile actuation. It also discusses the concept of localized haptic rendering, the selection of electrostatic actuation, human haptics and vibrotactile perception, the working principle of the electrostatic resonant actuator (ERA), and presents a summary of published studies on localized vibrotactile rendering and identified research gaps. Further, the mathematical preliminaries needed for this study are discussed.
- **Chapter 3:** This chapter focuses on introducing and constructing a narrow touch bar using electrostatic resonant actuators (ERAs). It explains the modeling process using the finite element (FE) method with flexible boundary conditions for the touch bar. The chapter also covers prototype development, experimental procedures, the method for localized haptic rendering, and an energy-based approach for managing vibrotactile feedback. Additionally, it presents a parametric study using the FE model for design considerations in achieving rich vibrotactile feedback.

- **Chapter 4:** This chapter focuses on the performance of a full-scale rectangular touch surface. It discusses the modeling process of the touch surface using the finite element (FE) method with flexible boundary conditions. The chapter also covers prototype development, experimental procedures, a method for localized haptic rendering, an energy-based approach for managing vibrotactile feedback, and a parametric study using the FE model to optimize design considerations for achieving rich vibrotactile feedback.
- **Chapter 5:** This chapter summarizes concluding remarks with contributions and future scopes of this study.

2. Background and Literature Review

This chapter introduces touch screen displays (TSDs) and their advantages over conventional displays, different haptic actuation methods available for TSDs with a light on the preferred actuation method (i.e., vibrotactile actuation), and the idea of localized haptic rendering and its management. Further, different actuators available for the vibrotactile actuation of TSDs are presented, highlighting the reason for selecting electrostatic actuation for this study. An overview of human haptics is explained with an emphasis on vibrotactile perception. In addition, the working principle of the electrostatic resonant actuator (ERA) used in this study is explained. Published studies on localized vibrotactile rendering and its management are investigated and summarized. Based on the study of published studies, gaps are presented. Finally, some mathematical preliminaries used in this study are discussed.

A touch user interface (TUI), such as a touchscreen display, is an input device that enables users to interact with the system by directly touching objects on display with their fingertip or a touch stylus [27]. A touchscreen display (TSD) is an interface for user interaction with a computer using fingers or styluses [28]. Touch interfaces are handy alternatives to physical input devices like a keyboard and mouse for navigating graphical user interfaces (GUIs). Touch screens are found everywhere in our daily lives as means of human-computer interaction (HCI) / human-machine interaction (HMI). They simplify things by eliminating external components such as buttons, switches, and dials, which are often bulky and inefficient. Touchscreen inputs also reduce the probability of component failure over time [13]. Figure 3(a) shows user interaction with computers/machines equipped with conventional display system. Users predominantly depend on the visual feedback offered by traditional display systems to engage with computers or machines. These displays usually feature screens that exhibit information or graphical user interfaces (GUIs). Users utilize external input devices like physical keyboards, mice, or trackpads to input commands or interact with the system. Users interacting with a conventional display receive haptic feedback through the external input devices. For example, pressing a physical key on a keyboard or clicking a mouse button provides a tactile response that confirms the user's action. A drawback of conventional displays is that users cannot directly manipulate or navigate the graphical user interface. Instead, they depend on indirect techniques like moving a cursor on the screen with a mouse and selecting options or elements by clicking. This absence of direct manipulation can hinder the efficiency and intuitiveness of user interactions, especially in tasks requiring precise positioning or fine control. Moreover, conventional displays exhibit constraints in terms of flexibility. The rigid layout and design of the graphical user interface on the screen can impede the customization or adaptability of the system to align with individual user preferences or specific tasks. Users typically have restricted control over how information is arranged or organized on display, which can have repercussions on productivity and user experience. Technological advancements have led to the development of TSDs to address this limitation. Figure 3(b) shows user interaction with computers/machines equipped with TSDs. In TSD-based HMI/HCI systems, users directly interact with the graphical elements on display by touching or gesturing, eliminating the need for external input devices like keyboards or mice. This direct manipulation provides a more intuitive and immersive user experience, allowing for increased flexibility and enhanced interaction capabilities. Furthermore, TSDs offer the possibility of integrating haptic feedback directly into the display. Haptic feedback involves using tactile sensations or vibrations to give users a realistic sense of touch. By incorporating haptic feedback into TSDs, users can receive

physical feedback while interacting with graphical elements on the screen. For instance, when a virtual button is pressed on the display, it can emit a gentle vibration or provide a tactile response, emulating the feeling of pressing an actual button. This integration of haptic feedback enhances the authenticity and immersion of user interactions.

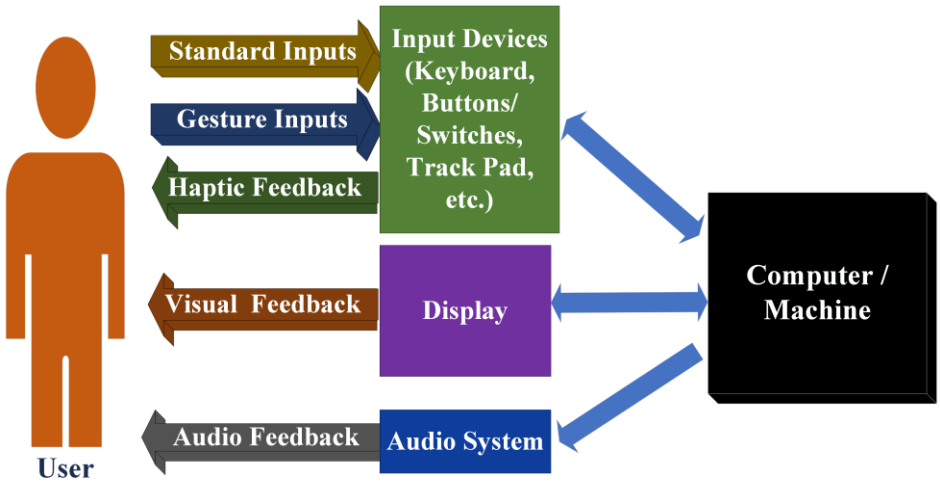

(a)

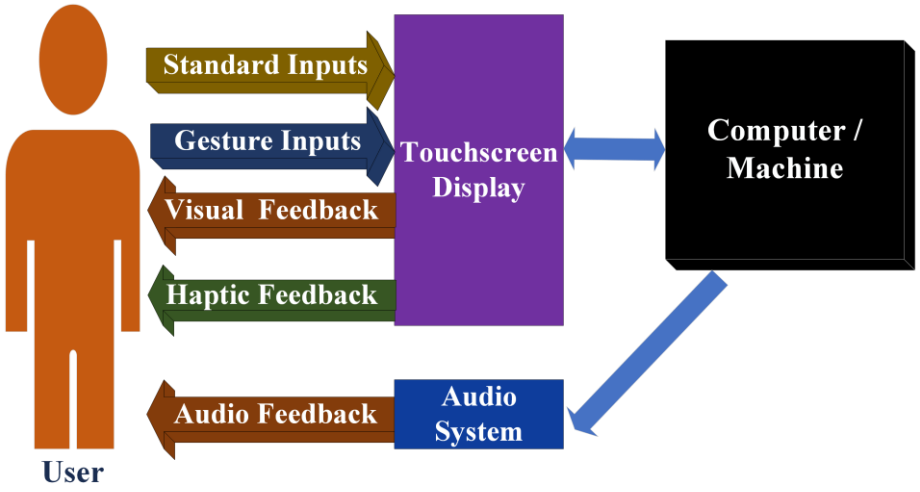

(b)

Figure 3: User interaction with computers/machines equipped with (a) traditional displays, and (b) touchscreen displays.

Touch screen displays for human computer interaction started with the development of light beam matrix input technology in IBM [29]. In 1972, a touch enabled computer, namely PLATO IV was developed for computer education [30]. Capacitive touch screen displays were introduced in 1985 [31]. Multi-touch sensing displays were introduced for tablet devices in [32]. Modern TSDs with multi-touch finger input have become available for consumers with the introduction of Apple iPhone in 2007 [1]. Following the success of the iPhone, TSDs of different dimensions and types become available in the market. TSDs are gaining increasing popularity in modern electronic devices due to their flexibility and the possibility of delivering other modes of interaction than audio and visual modes (e.g., gesture and haptic modes) [33] in the same interaction medium.

With technological advancements, consumers' needs are changing, and large touchscreen displays (TSDs) are entering people's lives [34]. One of the major uses of large TSDs is in personal computing devices like tablet computers, laptop computers, etc. Recently, displays of tablet devices have become larger, for example, Apple iPad Pro (~13 inches), Samsung Galaxy Tab S8 ultra (~ 14.6 inches), and Microsoft Surface Pro 8 (~13 inches). The display size of laptop pcs also reached about 16-17 inches size (e.g., Dell Inspiron 17 7000, Dell XPS, Apple MacBook Pro). A bigger display size provides a more involving experience for the user [1]. Further, touch screen displays (TSDs) are becoming increasingly popular in modern electronic devices for human-computer interaction (HCI)/human-machine interaction (HMI) due to their flexibility and the possibility of delivering other modes of interaction than audio and visual modes (e.g., haptic and gesture modes) [33].

2.1. Haptic Actuation of TSDs

Tactile haptic rendering involves replicating physical sensations perceived through touch, like the vibrations on a touchscreen [20]. On the other hand, kinesthetic haptic rendering aims to recreate the sense of movement and resistance, such as the force feedback in a 3D computer program. When combined, these two forms of rendering form haptic rendering, which encompasses all touch-based technologies. Tactile rendering provides rich, intuitive, and genuine information without the need for complex and costly mechanisms. Tactile actuation is often associated with haptic feedback in modern consumer products with TSDs [35]. This is because commercially available tactile actuators are compact, lightweight, and affordable, which makes it simple to incorporate tactile systems. Therefore, tactile actuation is attractive due to the additional information they provide without incurring significant expenses. There are generally three types of actuation methods found for tactile surfaces [36]:

- **Electro-tactile actuation**: this type of actuation makes electrical currents penetrate through the user's skin to activate the sensory nerves leading to tactile sensation. Depending on stimulation parameters, the user may feel insignificant feedback, and/or painful or uncomfortable sensations in electro-tactile stimulation. Moreover, the stimulation parameters causing a meaningful and uncomfortable sensation vary greatly from user to user. This makes the amplitude of electro-tactile displays be calibrated before each use case, which is not practical.
- **Electro-vibration actuation:** this method utilizes the electro-static effect by placing high-voltage electrodes under an insulating layer of the display. When the user places the finger on the display, the horizontal deformation of the skin is detected as a tactile sensation due to the skin's contact with the electrode and the relative movement of the finger. Electro-vibration method is limited by the fact that the user's finger needs to slide or move over the display to feel a haptic sensation and there is less variability of vibrations across the surface. Moreover, the perceived haptic feedback depends on external factors like humidity and temperature, and the user may feel an electric shock.
- **Mechanical/vibrotactile actuation:** this method incorporates various actuators for mechanical vibration of the surface. Mechanically actuated surfaces are free from the risk of electric shock and uncomfortable sensations. Given a suitable type of actuator, they are much simpler to develop compared to other types.

Among the different actuation methods, vibrotactile actuation has become the preferred choice for TSD applications due to its affordability, simplified design, and low power consumption[37]. Based on the size of TSDs used, vibrotactile rendering can be classified into two types as follows [20].

- **Monolithic Vibrotactile Rendering:** When utilizing a compact device with a small TSD, it is more advantageous to apply vibrations to the entire display rather than a specific section of it, as depicted in Figure 4(a). To accomplish this, one portion of the vibrating device should be firmly connected to the object, allowing the other part to move unrestrictedly. If the vibrating device is not securely affixed to the object, it will not effectively transfer the vibrations to the user's hands. Moreover, it is crucial for the object to possess rigidity and lack flexibility to ensure that the vibrations propagate throughout the entire device without being absorbed through bending.
- **Localized Vibrotactile Rendering:** When utilizing a device with a large TSD, it is recommended to employ a vibrotactile rendering method that focuses on vibrating one or more small regions, as depicted in Figure 4(b). Rather than relying on a rigid link, designers should strive for a lightweight and extremely flexible connection between the components responsible for delivering the vibrotactile signals and the remaining system.

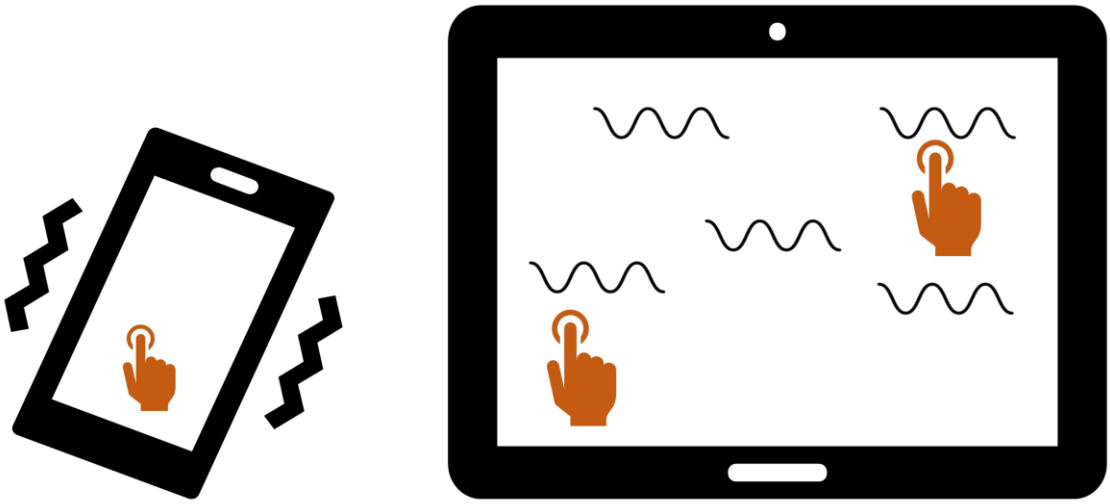

(a) (b)

Figure 4: Two types of vibrotactile rendering in TSDs based on display size: (a) monolithic vibrotactile rendering and (b) localized vibrotactile rendering.

As already stated, vibrotactile actuation has become a preferred choice for haptic devices with TSDs. The actuators available for vibrotactile haptic feedback generation are of the following types [19],[38]–[41].

- **Eccentric Rotary Mass (ERM) actuators:** In mobile devices, ERM actuators are mostly used. ERM actuators utilize the rotational motion of an unbalanced mass to provide vibrations.

- **Linear Resonant Actuators (LRAs) or voice coil actuators:** LRAs are small size actuators using electromagnet and spring mass systems to generate vibrotactile feedback.
- **Piezoelectric actuators:** Piezoelectric actuators utilize the inverse piezoelectric effect, whereby the application of an alternating current (AC) electric field to a piezoelectric material result in the generation of mechanical stress or deformation that is directly proportional to the electric field's intensity.
- **Electrostatic actuators:** Electrostatic actuators employ electrostatic attraction forces for creating vibrotactile sensations. In general, parallel plate electrode configuration is used in electrostatic actuators. The force of attraction in electrostatic actuators is directly proportional to the electrode area. Electrostatic actuators can be made in small and thin modules, making them desirable candidates for touch screen device applications.
- **Controllable fluid actuators:** These actuators use an overlay of controllable fluid such as magnetorheological (MR) fluid and electrorheological (ER) on the haptic surface. MR fluid-based actuators are actuated using an array of electromagnets. ER fluid-based actuators operate when an electric field is applied, which alters the viscous behavior of the fluid.
- **Electro-active polymer (EAP) actuators:** Electro-active polymers (EAP) are substances that experience notable transformations in their dimensions or structure when subjected to electrical stimulation. These materials have garnered considerable attention in the realm of haptic technologies due to their exceptional attributes, including remarkable responsiveness, flexibility, resistance to harm, energy efficiency, and lightweight nature.

The critical factors for a practical vibrotactile actuator suitable for large touch screen displays (TSDs) are rapid response time, minimal residual vibrations, low power usage, high vibration intensity, and appropriate size dimensions. ERM actuators have a slower response time (> 100 ms) and have the disadvantage of residual vibrations from the inertia of the mass. The application of ERM actuators is limited to small TSDs in smartphones, smartwatches, etc. The response time of LRAs is quicker (~ 20 ms) than the ERM actuators. However, LRAs are limited by their narrow bandwidth of vibrations and residual vibrations. Piezoelectric actuators have a very fast response time (~ 5 ms), and they can generate very short-duration vibrations (< 3 ms). However, piezoelectric actuators are limited by their high cost and high-power requirement. Parallel plate configurations are commonly used for electrostatic actuators, offering advantages such as rapid response, minimal residual vibrations, low power consumption, and compact size. However, these actuators are constrained in terms of vibration intensity due to the snap-in phenomenon, which restricts the range of displacement [16]. To overcome this limitation, a variation of electrostatic actuators called electrostatic resonant actuators (ERAs) with dual electrodes has been developed, proving to possess adequate vibration intensity suitable for large tactile sensory devices (TSDs) [19]. The response time of MR fluid is very fast (< 2 ms), and vibrations up to 600 Hz with arbitrary waveforms can be generated. MR fluid actuators are limited by the size of electromagnets used, and they can't be utilized in capacitive touch screens. ER fluid actuators offer the advantage of achieving high frequencies (approximately 1 kHz) during state transitions, making them valuable for haptic interfaces. However, a notable drawback is the elevated voltage demand (around 2-4 kV per millimeter electrode gap), which can potentially pose safety hazards to users. The production process for EAP actuators is intricate and not conducive to large-scale manufacturing, resulting in their limited availability in the market.

Despite the presence of various types of vibrotactile actuators, vibrotactile actuators capable of generating tactile sensations of sufficient intensity are not abundant [47]. This is because, with the increase in surface area, the vibrotactile feedback diminishes in magnitude for large touch screen displays [51]. As already stated, the most important parameters of a feasible actuator for large TSDs are fast response time, almost no residual vibrations, low power consumption, high vibration intensity, and compact dimensions. Among the different vibrotactile actuators, piezoelectric and electrostatic actuators are promising options for large TSDs. Piezo actuators are widely used for both small and large touch surfaces. However, the expensive nature of piezo actuators and high power requirements provide room for alternative options. Electrostatic actuators can be an alternative to piezo actuators because they offer rapid response, minimal residual vibrations, low power consumption, and are compact in size. As mentioned, recently developed electrostatic resonant actuators (ERAs) are found to be effectively rendering vibrotactile feedback on large TSDs [25], [41].

Multi-touch TSDs have become common in digital devices since their introduction in Apple iPhone (2007) [29]. Multi-user applications of large TSDs, like tabletop training, collaborative learning, etc., require haptic feedback at multiple points of a TSD. Multi-zone use scenario of a large TSD is shown in [4] for an automotive IVIS where the large TSD of the IVIS is divided into two zones (one for the driver and one for the passenger). In Neurological Music Therapy (NMT), multi-touch haptic feedback on large TSDs is required to enhance the sensory experience and improve engagement during the therapy session [6]. In TSD-based flight decks, for example, Boeing's 777-x, multi-zone segmentation of the displays allows for collaboration between the pilot and copilot, where both manipulate the same display to perform complex tasks [42]. Further, high-definition games played in large TSDs require multi-point haptic feedback throughout the surface to improve user input accuracy. For multi-user and multi-zone haptics, localized vibrotactile rendering in large TSDs needs to be controlled throughout the surface. Therefore, the problem of rendering vibrotactile feedback on large TSD becomes two-folded: localized vibrotactile feedback (The ability to generate vibrotactile feedback throughout the display) and management of localized vibrotactile feedback (The ability to position vibrotactile feedback at the desired locations of the display).

2.2. Overview of Human Haptics

Skin is the largest body part of humans, and skin surface is an expressive medium for transmitting information using touch [43]. Touch refers to the sensation felt when human skin is subjected to mechanical, chemical, thermal, or electrical stimuli. The word *haptic* finds its origin in the Greek word *haptesthai*, which means the sense of touch as the way humans recognize and interact with real-world objects and space [44]. Humans can explore and manipulate real world tasks using haptics. The sense of touch in the human body differs from the other four senses because it is not concentrated on a specific region of the body. In virtual worlds triggered by digital devices, the sense of touch needs to be artificially created for humans [45]. Human haptics can be generally divided into two types [45]: Kinesthetic sensations and Tactile/cutaneous sensations. Kinesthetic sensations are characterized by forces and toques, as depicted in Figure 5(a). Humans sense them in the joints, muscles, and tendons. Tactile/cutaneous sensations are characterized by vibrations, pressure, and shear, as depicted in Figure 5(b). Humans sense them using specialized sensory organs embedded in the skin.

The human kinesthetic system tracks limb positions, movements, and muscle tensions. This process is also termed as *proprioception*. The receptors engaged in kinesthetic sensing include muscle spindles, and Golgi tendon organs. Muscle spindles sense stretching muscle, and Golgi tendons sense the change in muscle tension. Exciting these receptors can produce the illusion of movement and/or force. The design and development of kinesthetic haptic devices is challenging due to the wide human dynamic range[45].

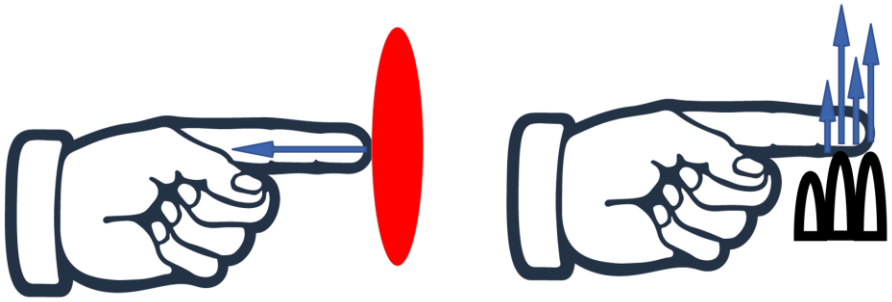

(a) (b)

Figure 5: Two modalities of human haptics: (a) kinesthetic sensations and (b) tactile/cutaneous sensations (adapted from [45]).

The specialized sensory organs used in cutaneous system are mechanoreceptors embedded in the skin [45]. The density of mechanoreceptors varies with the location on the body. They are denser in the glabrous skin of the hands and feet. Their density decreases in hairy skin. Therefore, tactile sensation is more pronounced on the glabrous skin. Skin mechanoreceptors can be broadly divided into two types [46] as shown in Figure 6: Rapidly Adapting (RA) Mechanoreceptors and Slowly Adapting (SA) Mechanoreceptors. RA Mechanoreceptors can be further classified into two types: Meissner Corpuscles and Pacinian Corpuscles. SA Mechanoreceptors can be further classified into two types: Merkel Cells and Ruffini Endings. The mechanoreceptors can sense vibrotactile stimulation in various sites of our body at frequencies 0.4-1000 Hz [47]. Based on experiments with human subjects using sinusoidal vibratory displacements, Human vibrotactile perception through glabrous skin uses four distinct channels [48]: P Channel (Pacinian Channel: Pacinian corpuscle and fibers are responsible for this channel. This channel can sense vibrations in the range of 40 – 1000 Hz. The lower limit of sensing can also be 30 Hz [47]), NP-I Channel (non-Pacinian-I Channel: Meissner corpuscles and RA fibers are responsible for this channel. This channel primarily senses fluttering sensations in the 3-40 Hz frequency range.), NP-II Channel (non-Pacinian-II Channel: Ruffini endings and SA II fibers are responsible for this channel. This channel primarily senses buzzing sensations in the 100-1000 Hz frequency range. Practically, for providing sensory input required for gripping and holding objects.), and NP-III (non-Pacinian-III channel: Merkel Cells and SA I fibers are responsible for this channel. This channel primarily senses pressure in the frequency range of 0.4-3 Hz. Practically, useful for detecting surface topography.).

The relationship between the minimum vibration amplitude needed to detect vibration (detection threshold) and the stimulation frequency is a way to determine the maximum limit of sensory resolution on the skin [47]. Several studies were done using sinusoidal displacement amplitudes at different frequencies with human subjects up to 500 Hz to characterize the skin vibration detection threshold at various parts of the body [46], [49], [50]. The optimal sensitivity

(lowest threshold) is found at most of the body sites at frequencies 150-300 Hz. The amplitude detection threshold observed in each study agreed with a V-shaped curve with a minimum at a frequency of ~320 Hz. Figure 7 shows the human vibrotactile detection threshold as peak amplitudes with change in excitation frequencies from [49]. We observe that at low frequencies, the detection threshold is higher. The detection threshold keeps decreasing as we increase the frequency until it reaches the minimum at a frequency of ~320 Hz. Beyond that minimum detection threshold frequency, the detection threshold further increases by a marginal amount.

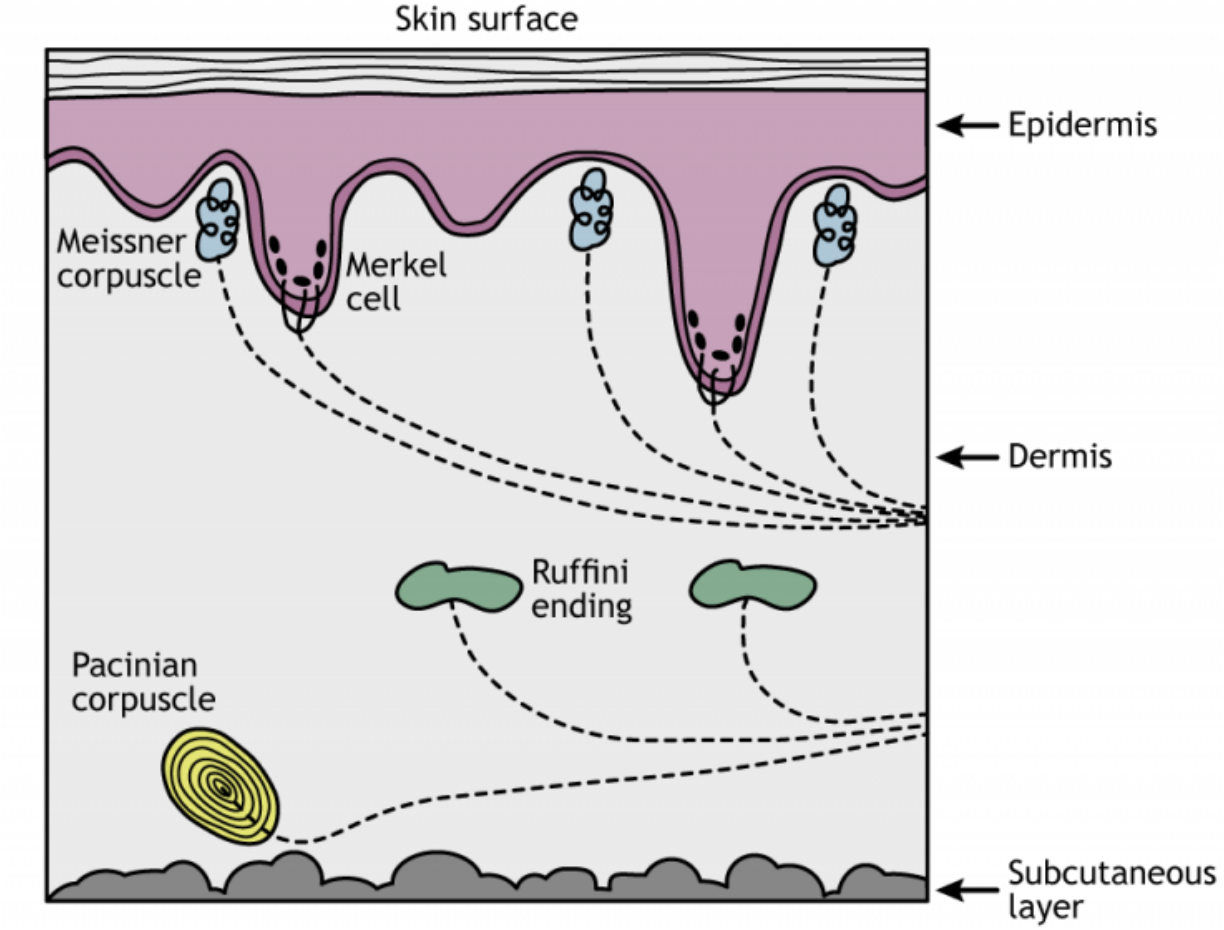

Figure 6: mechanoreceptors in the glabrous skin [51].

While academic literature typically expresses the minimum vibration needed to detect a tactile sensation in terms of displacement amplitude, the industry commonly uses acceleration amplitude [50]. In the industry, standard vibration amplitudes for vibrotactile measurement are expressed in g (1 g = 9.8 m/s^2) [52]. The minimum acceleration detection threshold at fingertip is found between 80-160 Hz in existing literature [50], [52]. Figure 8 shows the human vibrotactile detection threshold as peak accelerations with change in excitation frequencies from [50]. The trend of detection thresholds in terms of peak accelerations with change in frequencies is slightly different from the detection thresholds in terms of peak amplitudes. From 10 Hz frequency, the detection threshold increases marginally and starts to decrease beyond 40 Hz till it reaches minimum at ~160 Hz frequency. After the minimum point, the detection threshold abruptly increases.

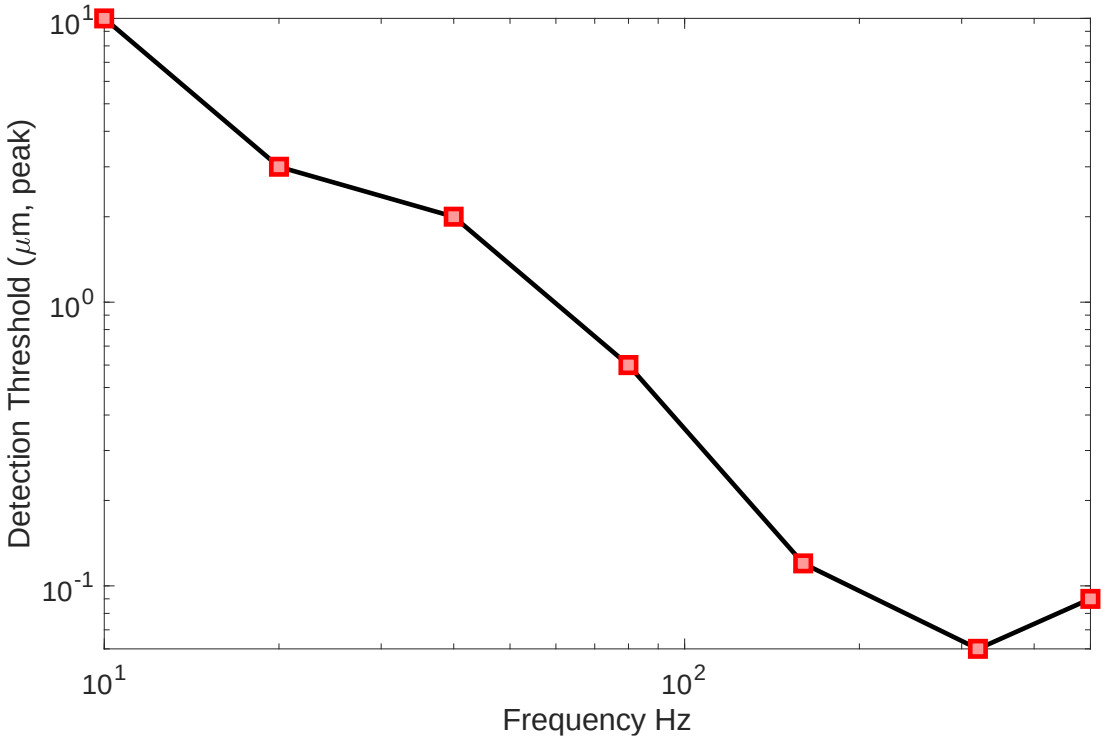

Figure 7: Vibrotactile detection threshold at fingertip in terms of peak amplitude with frequencies of excitation (adapted from [49])

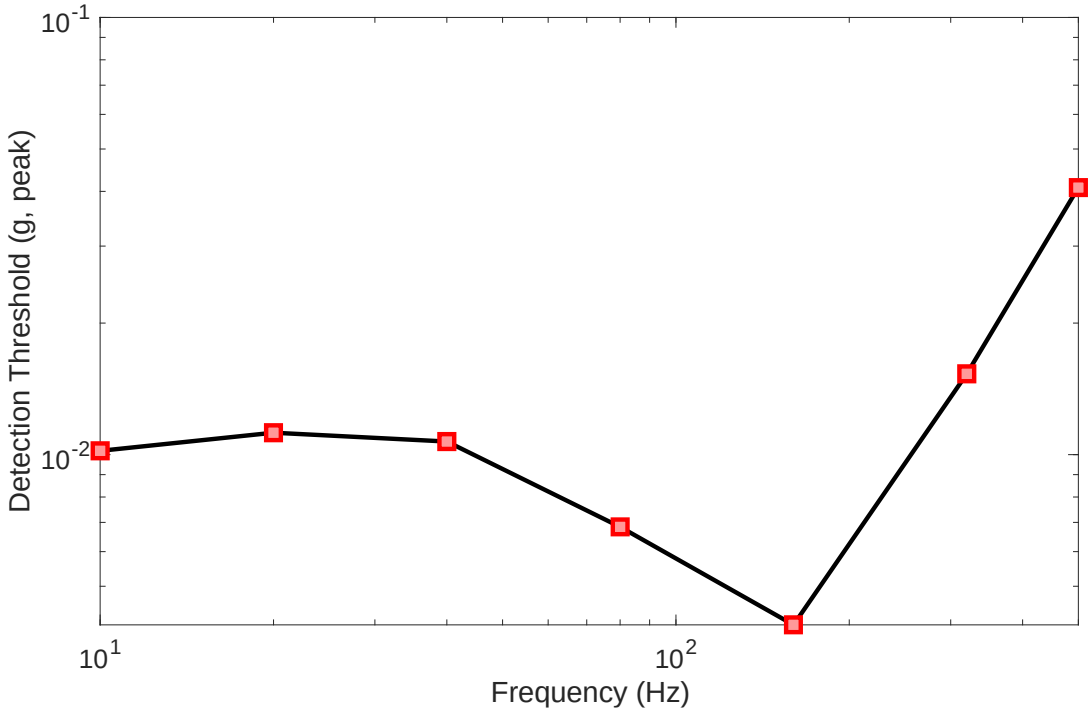

Figure 8: Vibrotactile detection threshold at fingertip in terms of peak acceleration corresponding to excitation frequencies (adapted from [50]).

2.3. Electrostatic Resonant Actuator (ERA)

Electrostatic actuators utilize the interaction between two conducting electrodes when an electric voltage is applied, leading to different types of actuators based on their electrode configuration [53]. Electrostatic parallel plate actuators offer a viable solution for generating haptic feedback in touch screen devices [54]. Their functionality resembles that of a Linear Resonant Actuator (LRA), with the distinction that they employ electrostatic force instead of electromagnetism. Typically, these actuators consist of two parallel plate electrodes, where one electrode is affixed to a surface, while the other is allowed to move in a single direction towards or away from the fixed electrode. Like the movable mass in an LRA, the movable electrode is supported by one or more springs, which generate a restoring force. Upon applying a voltage across the electrodes, an electrostatic attractive force emerges between them, drawing the movable electrode closer to the fixed one. Electrostatic forces are generally perceived as relatively weak and have predominantly been utilized in MEMS (Micro-Electro-Mechanical Systems) applications. However, in principle, the strength of the electrostatic force escalates in proportion to the surface area of the electrode [54]. This implies that electrostatic actuators have the potential to be designed for large-TSDs, delivering tactile sensations of adequate intensity to the user. However, electrostatic actuators have a major disadvantageue to a phenomenon called snap-in [54]. Parallel plate electrostatic actuators experience a non-linear relationship between the force exerted on the plates and the spacing between them. But the restoring force, which determines the actuator's displacement, generally follows a linear pattern. This linear relationship imposes a limitation on the range of parallel-plate actuators, typically confining it to around one-third of the gap between the plates. If the deflection exceeds this limit, a phenomenon occurs where the required voltage to maintain the displacement increases much faster than the restoring force. As a result, the plates abruptly come into contact, or snap together. If no insulating layer is present, this contact can lead to a short circuit. The study in [55] introduced a novel electrostatic actuator called the electrostatic resonant actuator (ERA) designed specifically for large touchscreen devices. The researchers utilized a single stationary electrode that received high voltage inputs, along with a movable mass, to enhance the intensity of vibrations. Through the utilization of the beat phenomenon, which arises from the interaction of two high voltage input signals applied to the electrode, they successfully showcased the potential of this actuator for use in large display applications. However, with a single fixed electrode configuration, the displacement of the ERA is still limited to one-third of the air gap due to which beat phenomenon was used to generate vibrotactile feedback of sufficient intensity in [55]. A new ERA with two fixed electrodes, termed dual-electrode ERA, is proposed in [25], the schematic of which, along with an exploded-view, is shown in Figure 9. This dual-electrode ERA generates vibrotactile feedback of significantly higher intensity compared to the single fixed electrode ERA. In [41], the feasibility of the dual-electrode ERA for large bar-type TSD is presented.

The dual-electrode ERA consists of three main components: a central inertial mass and two fixed electrodes on each side, as shown in Figure 9. The dual-electrode name comes from the fact that the ERA has two fixed electrodes where we apply electric potential. Unlike conventional electrostatic actuators, the ERA module employs a grounded moving mass to enhance vibration intensity. The mass, suspended between the electrodes by radial beam springs, undergoes oscillations within the actuator. This oscillation is made possible by an air gap between the suspended mass and the electrodes. In the ERA, the grounded mass can be considered a neutral object, and the fixed electrodes can be considered charged objects. Within the module, the

electrodes function as charged objects, while the stainless-steel grounded mass acts as a neutral conductive object. There are two spacers used on both sides of the grounded mass to separate it from the electrodes. When a high voltage input is applied to one of the electrodes, a capacitance is formed between the grounded mass and the electrode, generating an electrostatic force that attracts the mass towards the electrode. The mass is then pulled towards the electrode, but the radial beam springs exert a restoring spring force to bring it back to its equilibrium position. This rapid fluctuation of forces induces oscillations in the mass, resulting in the vibration of the actuator. To prevent any interference between the electrostatic forces generated by each electrode, it is necessary to activate the two electrodes in an alternating manner, but not simultaneously. The oscillations of the mass can be connected to TSDs for rendering vibrotactile feedback as shown in Figure 9. Details on the construction and working of the ERA are explain thoroughly in [19], [25].

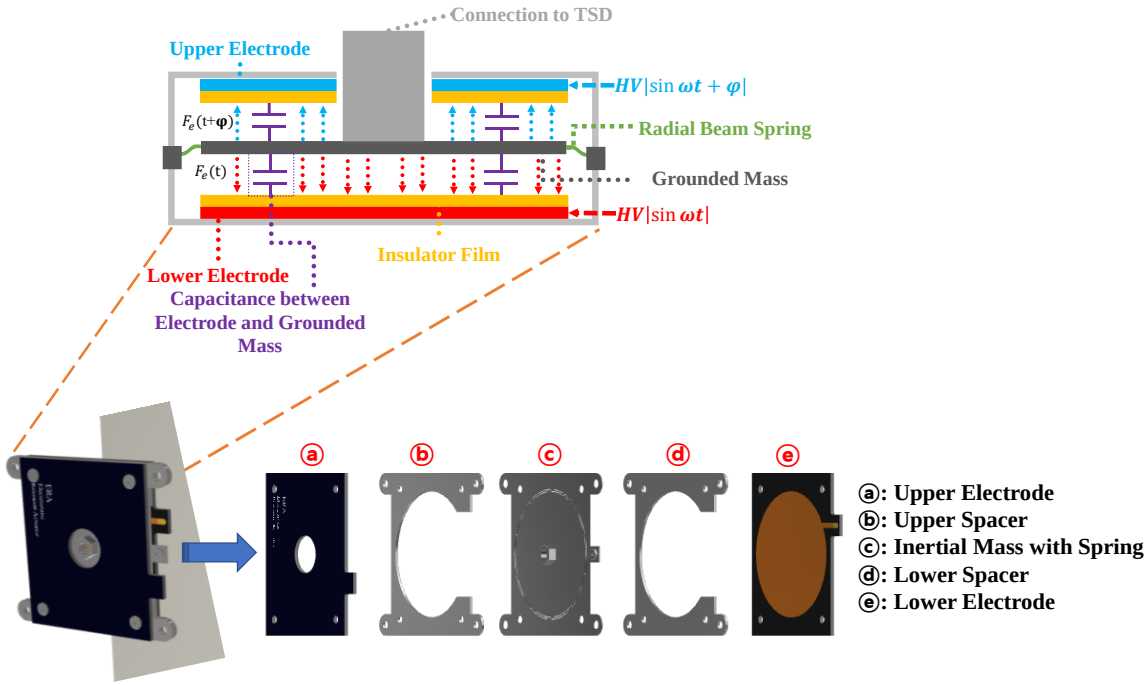

Figure 9: The schematic and working principle of the dual-electrode ERA (adapted from [25])

2.4. Localized Vibrotactile Feedback and Its Management

With feasible actuators for large TSDs, it is still challenging to render vibrotactile feedback throughout the display (localized vibrotactile feedback), as it is difficult to shape the waves propagating through a TSD [38]. Using rigid boundaries for TSDs under vibrotactile actuation often results in dead zones or areas with minimal haptic feedback [26]. The presence of dead zones or nodes on a TSD with rigid boundaries can be attributed to the fact that shaping the mode shapes of the touch surface is not convenient, or it may require a drastic change in excitation frequencies, which sometime may be beyond perceptible human range (>1000 Hz) [25]. Existing literature employs many actuators with rigid boundaries to eliminate dead zones or nodes on large TSDs, Existing [26], [56]–[63]. Flexible connections at the boundaries of the TSDs are recommended for effective localized haptic rendering [20]. Further, multi-frequency excitation (excitation with desperate frequencies of the actuators) may aid in conveniently controlling the mode shapes of a

large TSD with excitation frequencies in the perceptible human range, which is not explored in the existing literature.

As already stated, existing methods for localized vibrotactile rendering on large TSDs utilize numerous actuators due to the inherent difficulty in shaping waves propagating through the TSDs and the use of rigid boundary conditions. The use of many actuators is often impractical for commercial purposes due to size, form factor, and power supply constraints [57]. In [41], the possibility of localized vibrotactile rendering using a limited number of actuators is experimentally shown for a bar-type display with flexible boundaries. However, the study in [41] does not generalize to commonly used large TSDs. Localized vibrotactile rendering with numerous actuators using the eigenfunction superposition method is discussed in [56]. However, the excitation frequencies used in [56] are in the ultrasonic frequency range, beyond the human perceptible vibration range. In [57], localized haptic rendering using the time-reversal wave focusing method with a restricted number of actuators is presented. However, the response time of the method presented in [57] is slower for practical implementation, and the excitation frequencies are also in the ultrasonic range. With numerous actuators, localized vibrotactile feedback is generated using time reversal wave focusing in [26], [58]. Therefore, there is a need to explore localized vibrotactile rendering on large TSDs with a restricted number of actuators and flexible boundaries.

Multi-touch or multi-zone vibrotactile haptic rendering requires management of the rendered localized haptic feedback for large TSDs [60]. Even though localized vibrotactile feedback is generated in a large TSD, management or positioning of the generated feedback is still difficult due to the need to control waves traveling through the TSD [19]. One approach to controlled localized vibrotactile rendering is the confinement of vibrotactile stimulation above the actuator and populating the TSD with numerous actuators to precisely control the rendered feedback [59]. However, with numerous actuators comes the constraint of space and power consumption for practical considerations. In [60], the control of the rendered localized vibrotactile feedback is discussed using the inverse-filter method. However, the study in [60] also uses numerous actuators. The control of rendered localized vibrations in the 200-300 Hz range is reported to be achieved with many actuators using a generalized adversarial network (GAN) which generates time-reversed signals [61]. Superimposition of vibration modes with numerous actuators is discussed with reasonable positioning of the rendered localized vibrotactile feedback in [62], [63]. Therefore, there is room for exploring the management of rendered localized vibrotactile feedback in large TSDs with a limited number of actuators.

Localized vibrotactile rendering using transparent electrode display panels is presented in [64], [65]. In such panels, transparent electrodes are attached to the display in a parallel plate fashion and are excited with high voltage to provide electrostatic actuation. A multi-modal haptic feedback generation strategy (electro-vibration and mechanical vibration) is presented in [64]. The study in [65] achieved management of the rendered haptic feedback using an energy-based method. However, with transparent electrode display panels, the intensity of generated vibrotactile feedback is not sufficiently rich for large TSD applications [55]. Furthermore, modularizing the design of displays for different sizes of TSDs is a challenging task.

Vibrotactile haptic stimulation on large TSDs with a restricted number of actuators depends on factors like the type of actuators used, the type of excitations, the boundaries used, and the placement of the actuators [66]. Physically constructing different large TSD systems with different configurations of these factors is impractical. The development of mathematical models for large TSD systems can aid in the exploration of localized vibrotactile feedback on large TSDs with a restricted number of actuators. Such mechanical simulation models of large TSDs also allow us to extend one haptic rendering method to different materials and actuators, find a suitable number of actuators and their positioning, and find ways of better localization [66]. Finite element modeling of touch surfaces has been discussed with piezo actuators in [67]–[70], focusing on generating maximum vibration amplitude on the touch surface and not managing localized vibrotactile feedback. Further, the literature lacks an exploration of modeling strategies for multi-frequency excitations, where actuators operate at different frequencies during stimulation. Moreover, a dearth of model-based studies offer design considerations specifically for the haptic actuation of large TSDs. Designing effective and efficient haptic systems for large TSDs requires careful consideration of various factors, such as actuator type, touch surface material, and actuator configurations. Mathematical models can be valuable in guiding the design process, planning the actuator layout, and facilitating better localization capabilities.

2.5. Identified Gaps

Based on the literature review, the following are the gaps that must be addressed.

- The literature does not address localized vibrotactile haptic rendering in large TSDs with flexible boundary conditions.
- Using a limited number of vibration actuators for localized vibrotactile stimulation in large TSDs poses a significant challenge not adequately addressed in the existing literature.
- Mathematical model development of TSD systems, with haptic rendering capabilities, in a way such that a haptic rendering method can be extended to different actuator types, touch surface material, and actuator configurations is not properly addressed in the literature. Existing model-based studies do not cater to variable excitation parameters such as frequencies of excitations of the actuators.
- Using a restricted number of vibration actuators, the management or positioning of localized haptic rendering in large TSDs is mostly non-existent in the literature.
- There is a lack of model-based study allowing for design considerations in the design of vibrotactile haptic devices with large TSDs.

The literature review reveals significant gaps in the current understanding and exploration of localized vibrotactile haptic rendering in large TSDs. These gaps include the lack of attention to flexible boundary conditions, the challenges associated with using a restricted number of vibration actuators for localized stimulation, and the absence of comprehensive mathematical models that can be extended to different actuator types, touch surface materials, and configurations. Additionally, the management and positioning of localized haptic rendering, as well as the lack of model-based studies offering design considerations for large TSDs, haptic rendering with multi-frequency excitations are notable areas that need to be addressed. Closing these gaps through further research and development will contribute to the advancement of vibrotactile haptic rendering in large TSDs, leading to enhanced user experiences in various applications.

2.6. Mathematical Preliminaries

This section discusses some mathematical methods and preliminary information that will be repeatedly used in future chapters.

2.6.1. Response of multiple-DOF systems with multiple excitation frequency

Finite-element methods, when applied to dynamic linear elasticity problems, give rise to a system of differential equations. Typically, such systems of differential equations are coupled multiple-DOF (degrees of freedom) second order differential equations expressed in matrix form as,

$$\mathbf{M}\ddot{\mathbf{x}}(t) + \mathbf{C}\dot{\mathbf{x}}(t) + \mathbf{K}\mathbf{x}(t) = \mathbf{f}(t) \tag{1}$$

Here, $\mathbf{M}, \mathbf{K}, \mathbf{C}$ and $\mathbf{f}$ are mass, spring, damping, and force matrices coming from discrete finite-element models. Further, $\mathbf{x}$ is the vector containing displacements at each degree of freedom. If the input forces are harmonic in nature, for m harmonic excitations, the force vector can be expressed as,

$$\mathbf{f}(t) = \sum_{i=1}^{m} \left(\mathbf{g}_i \sin \omega_i t + \mathbf{h}_i \cos \omega_i t \right) \tag{2}$$

Here, $\mathbf{g}_i$, $\mathbf{h}_i$ are constant vectors with amplitudes of the harmonic excitations at different degrees of freedom.

2.6.1.1. Approximating response using numerical solvers

Computing environments like MATLAB, Python, etc. provide standard numerical solvers that can solve a system of first-order differential equations. We have to convert the system of second order differential equations in (1) into a state space form with first order equations so that we can feed it to numerical solvers available in various computing environments. For an n-DOF system of 2nd order differential equations, we require 2n state variables. We define the state vector as $\begin{bmatrix} \mathbf{x} & \dot{\mathbf{x}} \end{bmatrix}^T$. Therefore, the state equations of (1) are written as,

$$\begin{aligned} \dot{\mathbf{x}} &= \mathbf{0}_{\text{nxn}}\mathbf{x} + \mathbf{I}_{\text{nxn}}\dot{\mathbf{x}} \\ \ddot{\mathbf{x}} &= -\mathbf{M}^{-1}\mathbf{K}\mathbf{x} + -\mathbf{M}^{-1}\mathbf{C}\dot{\mathbf{x}} + \mathbf{M}^{-1}\mathbf{f} \end{aligned} \tag{3}$$

In matrix form, we can rewrite equation (3) as,

$$\underbrace{\begin{bmatrix} \dot{\mathbf{x}} \\ \ddot{\mathbf{x}} \end{bmatrix}}_{\dot{\mathbf{z}}} = \underbrace{\begin{bmatrix} \mathbf{0}_{\text{nxn}} & \mathbf{I}_{\text{nxn}} \\ -\mathbf{M}^{-1}\mathbf{K} & -\mathbf{M}^{-1}\mathbf{C} \end{bmatrix}}_{\mathbf{A}} \underbrace{\begin{bmatrix} \mathbf{x} \\ \dot{\mathbf{x}} \end{bmatrix}}_{\mathbf{z}} + \underbrace{\begin{bmatrix} \mathbf{0}_{\text{nx1}} \\ \mathbf{M}^{-1}\mathbf{f} \end{bmatrix}}_{\mathbf{B}} \tag{4}$$

(4) is in state space form and can be written in compact form as,

$$\dot{\mathbf{z}} = \mathbf{A}\mathbf{z} + \mathbf{B} \tag{5}$$

Numerical solvers like MATLAB's *ode45* to solve for (5) and obtain the solution $\mathbf{z}$ which will contain the time dependent displacements and velocities for the system modeled as a system of multiple-DOF coupled second order differential equations.

2.6.1.2. Proposed analytical solution for vibrotactile response

Using (1) & (2), we write the system of differential equations describing a finite-element model with m harmonic excitations as,

$$\mathbf{M}\ddot{\mathbf{x}}(t) + \mathbf{C}\dot{\mathbf{x}}(t) + \mathbf{K}\mathbf{x}(t) = \sum_{i=1}^{m} \left(\mathbf{g}_i \sin \omega_i t + \mathbf{h}_i \cos \omega_i t \right) \tag{6}$$

Let the initial conditions be,

$$\mathbf{x}(0) = \mathbf{x_0}, \ \dot{\mathbf{x}}(0) = \mathbf{v_0} \tag{7}$$

The system response is the combination of free or homogeneous response $\mathbf{x}_H(t)$ and the forced or particular response $\mathbf{x}_P(t)$. $\mathbf{x}_H(t)$ is the solution of (8) and $\mathbf{x}_P(t)$ is the solution of equation (9). $\mathbf{x}_P(t)$ can be considered as the combination of all individual harmonic excitation responses $\mathbf{x}_{P_i}(t)$ as shown in (10).

$$\mathbf{M}\ddot{\mathbf{x}}_H(t) + \mathbf{C}\dot{\mathbf{x}}_H(t) + \mathbf{K}\mathbf{x}_H(t) = 0 \tag{8}$$

$$\mathbf{M}\ddot{\mathbf{x}}_p(t) + \mathbf{C}\dot{\mathbf{x}}_p(t) + \mathbf{K}\mathbf{x}_p(t) = \sum_{i=1}^{m} \left(\mathbf{g}_i \sin \omega_i t + \mathbf{h}_i \cos \omega_i t \right) \tag{9}$$

$$\mathbf{x}_P(t) = \sum_{i=1}^{m} \mathbf{x}_{P_i}(t) \tag{10}$$

Therefore, the total response of the system with multiple harmonic excitations is given as,

$$\mathbf{x}(t) = \mathbf{x}_H(t) + \mathbf{x}_P(t) = \mathbf{x}_H(t) + \sum_{i=1}^{m} \mathbf{x}_{P_i}(t) \tag{11}$$

We assume a particular solution of the form,

$$\mathbf{x}_P(t) = \sum_{i=1}^{m} \mathbf{x}_{P_i}(t) = \sum_{i=1}^{m} \left(\mathbf{p}_i \cos \omega_i t + \mathbf{q}_i \sin \omega_i t \right) \tag{12}$$

Here, $\mathbf{p}_i, \mathbf{q}_i$ are constant vectors representing the harmonic motion with the same frequency ω_i of the exciting force at *k*-th degree of freedom having different amplitude p_k and/or q_k of oscillations. Such a motion occurs at steady state when transient response of the system dies out. For i^{th} excitation, the steady state response is of the form,

$$\mathbf{x}_{Pi}(t) = \mathbf{p}_i \cos \omega_i t + \mathbf{q}_i \sin \omega_i t \tag{13}$$

Substituting (13) in (9), we obtain,

$$\begin{aligned} -\omega_i^2 \mathbf{M}\mathbf{p}_i \cos \omega_i t - \omega_i^2 \mathbf{M}\mathbf{q}_i \sin \omega_i t - \omega_i \mathbf{C}\mathbf{p}_i \sin \omega_i t \; + \omega_i \mathbf{C}\mathbf{q}_i \cos \omega_i t + \\ \mathbf{K}\mathbf{p}_i \cos \omega_i t + \mathbf{K}\mathbf{q}_i \sin \omega_i t = \; \mathbf{g}_i \sin \omega_i t + \mathbf{h}_i \cos \omega_i t \end{aligned} \tag{14}$$

Comparing coefficients of both sides of (14), we obtain the following matrix form,

$$\begin{bmatrix} \mathbf{K} - \omega_i^2 \mathbf{M} & \omega_i \mathbf{C} \\ -\omega_i \mathbf{C} & \mathbf{K} - \omega_i^2 \mathbf{M} \end{bmatrix} \begin{pmatrix} \mathbf{p}_i \\ \mathbf{q}_i \end{pmatrix} = \begin{pmatrix} \mathbf{h}_i \\ \mathbf{g}_i \end{pmatrix} \tag{15}$$

$\mathbf{p}_i, \mathbf{q}_i$ for a given excitation can be obtained whenever the left-hand side of (15) is not singular. The particular response due to i^{th} harmonic excitation is thus obtained as in (13). The total particular response is obtained by solving for each one of the m harmonic excitations and superposition of all of them as in (12). The singularity of the left-hand side of (15) implies that the system is in resonance and there is no steady state response as the vibrations increase without bound.

A homogeneous solution of (8) is a quadratic eigenvalue problem. We can use numerical solvers, for example, MATLAB®'s *eig* to compute associated eigenvalues and eigenvectors after converting (8) to a suitable state space eigenvalue form as shown in

$$\left(\underbrace{\begin{pmatrix} \mathbf{0} & \mathbf{I} \\ -\mathbf{M}^{-1}\mathbf{K} & -\mathbf{M}^{-1}\mathbf{C} \end{pmatrix}}_{\mathbf{A}} - s \underbrace{\begin{pmatrix} \mathbf{I} & \mathbf{0} \\ \mathbf{0} & \mathbf{I} \end{pmatrix}}_{\hat{\mathbf{I}}} \right) \underbrace{\begin{pmatrix} \mathbf{x}_H \\ s\mathbf{x}_H \end{pmatrix}}_{\mathbf{v}} = \begin{pmatrix} \mathbf{0} \\ \mathbf{0} \end{pmatrix} \tag{16}$$

We solve the generalized eigenvalue problem in (16) and obtain the eigenvector matrix $\mathbf{V}$ as in (17) with $\mathbf{r_1}, \mathbf{r_2}, \cdots, \mathbf{r_{2n}}$ be the eigenvectors associated with complex eigenvalues $s_1, s_2, \cdots, s_{2n}$ respectively.

$$\mathbf{V} = \begin{bmatrix} \mathbf{r}_1 & \mathbf{r}_2 & \cdots & \mathbf{r}_{2n} \\ s_1\mathbf{r}_1 & s_2\mathbf{r}_2 & \cdots & s_{2n}\mathbf{r}_{2n} \end{bmatrix} \tag{17}$$

Considering that the 2n eigenvectors span the state space in a sense that $\mathbf{V}$ is invertible, we get the homogeneous response of the touch bar system as,

$$\mathbf{x}_H(t) = \sum_{j=1}^{2n} a_j \mathbf{r}_j e^{s_j t} \tag{18}$$

The complete solution for a multiple degrees of freedom discrete finite-element model is given as,

$$\mathbf{x}(t) = \sum_{i=1}^{m} \left(\mathbf{p}_i \cos \omega_i t + \mathbf{q} \sin \omega_i t \right) + \sum_{j=1}^{2n} a_j \mathbf{r}_j e^{s_j t} \tag{19}$$

Using initial conditions from (7) in (19), we obtain (20). (20) can be written in matrix form as given in (21).

$$\begin{aligned} \mathbf{x}(0) = \mathbf{x}_0 &= \sum_{i=1}^{m} \mathbf{p}_i + \sum_{j=1}^{2n} a_j \mathbf{r}_j \\ \dot{\mathbf{x}}(0) = \mathbf{v}_0 &= \sum_{i=1}^{m} \omega_i \mathbf{q}_i + \sum_{j=1}^{2n} a_j s_j \mathbf{r}_j \end{aligned} \tag{20}$$

In (21), $\mathbf{V}$ is given by (17) and $\mathbf{a} = \begin{bmatrix} a_1 & a_2 & \cdots & a_{2n} \end{bmatrix}^T$ gives the coefficients a_j in (18). $\mathbf{a}$ is obtained from (21) whenever $\mathbf{V}$ is invertible.

$$\mathbf{V}\mathbf{a} = \begin{pmatrix} \mathbf{x}_0 - \sum_{i=1}^{m} \mathbf{p}_i \\ \mathbf{v}_0 - \sum_{i=1}^{m} \omega_i \mathbf{q}_i \end{pmatrix} \tag{21}$$

Therefore, the complete solution for displacements of a discrete finite-element is given by (19) . The steady state accelerations at different nodal positions for a discrete finite-element model can be given as,

$$\mathbf{\Phi}(t) = \ddot{\mathbf{x}}_P(t) = -\sum_{i=1}^{m} \omega_i^2 \left(\mathbf{p}_i \cos \omega_i t + \mathbf{q} \sin \omega_i t \right) \tag{22}$$

Therefore, the absolute peak steady-state amplitude of acceleration at any degree of freedom *k* of a discrete finite-element model can be obtained as,

$$\Phi_k == \sum_{i=1}^{m} \omega_i^2 \sqrt{\left(p_k\right)_i^2 + \left(q_k\right)_i^2} \tag{23}$$

(19) gives the complete solution of a multiple degree of freedom discrete finite-element model as a second-order coupled set of differential equations. Subsequently, we can obtain the peak steady-state amplitude of acceleration at any desired degree of freedom using (23).

2.6.1.3. Comparison between numerical and analytical solution strategies

In our study, we conducted a comprehensive comparison between the standard solution method and the proposed solution method within the MATLAB environment. The objective was to solve a system of multiple-DOF (degrees of freedom) second-order differential equations subjected to harmonic excitation. To evaluate the performance of the two methods, we generated random matrices M, C, K, and F with varying degrees of freedom. The excitation angular frequency was set at 60 rad/s for all cases. The results of our comparison are summarized in Table 1, providing valuable insights into the computational efficiency (in terms of time taken for computation) of the standard numerical and the proposed analytical solutions.

Additionally, Figure 10 visually represents the trends observed in the time taken for computation as the degrees of freedom increase. We observed a significant difference in the computational time between the two methods as the system's degrees of freedom increased. Specifically, the time required to solve the system increased abruptly with the numerical method, displaying a convex downward trend as illustrated in Figure 10. This behavior implies that the computational time exponentially grows with the degrees of freedom, reaching prohibitive levels for larger systems. Conversely, the proposed method demonstrated a distinct advantage in terms of computational efficiency. We noticed that the time required to solve the system using this method exhibited an approximately linear trend, as clearly depicted in Figure 10. This linear relationship indicates that the proposed method maintains a consistent and predictable computational time even as the degrees of freedom increase. The key finding was the substantial disparity in computation times between the two methods when dealing with systems having 20 or more degrees of freedom. When applied to such complex systems, the standard numerical solution method often took several seconds or even minutes to provide a solution. In contrast, the proposed analytical solution method was greatly efficient, delivering results within a fraction of a second even with degrees of freedom over 20. These findings highlight the advantage of the proposed method over the numerical approach in terms of computational efficiency when solving systems with a large number of degrees of freedom. By significantly reducing the computational time, the proposed method offers substantial practical advantages.

To demonstrate the effectiveness of the proposed method, we conducted a comparative analysis using a 20 degrees of freedom (DOF) system. For this purpose, we employed the same mass (**M**), damping (**C**), and stiffness (**K**) matrices as in Table 1. Additionally, we subjected the system to a harmonic excitation with a unity amplitude and a frequency of 60 Hz, applied at the first and last DOFs. In order to evaluate the accuracy of the proposed method, we solved the 20 DOF second-order system of differential equations using both the numerical method (employing the ode45 solver) and the proposed analytical method within the MATLAB environment. Our focus was on comparing the computed displacements at the 4^{th} and 18^{th} DOFs, as shown in Figure 11. To assess the quality of the solutions obtained, we computed the percentage error between the results obtained from the two methods at each time step. For the analysis, we considered a time period of 5 seconds with a time step of *1 ms*. Our findings revealed that the percentage error

between the computed displacements at the 4th and 18th DOFs was consistently 0.1% or lower at each time step. This outcome demonstrates the accuracy and efficacy of the proposed solution method for solving coupled second-order differential equations with multiple DOFs.

In summary, the proposed analytical method for solving second order multi-DOF systems of differential equations with harmonic excitations can solve the same with great efficiency and efficacy when compared to the numerical solution method.

Table 1: Comparison of solution computation time of the numerical method (ode45 solver in MATLAB) and the proposed analytical method with the increase in the DOFs

Degrees of Freedom	**Time taken using the numerical solution method using *ode45 (sec.)***	**Time taken using the analytical solution method (sec.)**
4	0.141	0.01
8	0.230	0.02
16	0.906	0.04
20	6.098	0.06
40	36.32	0.09
60	151.23	0.12

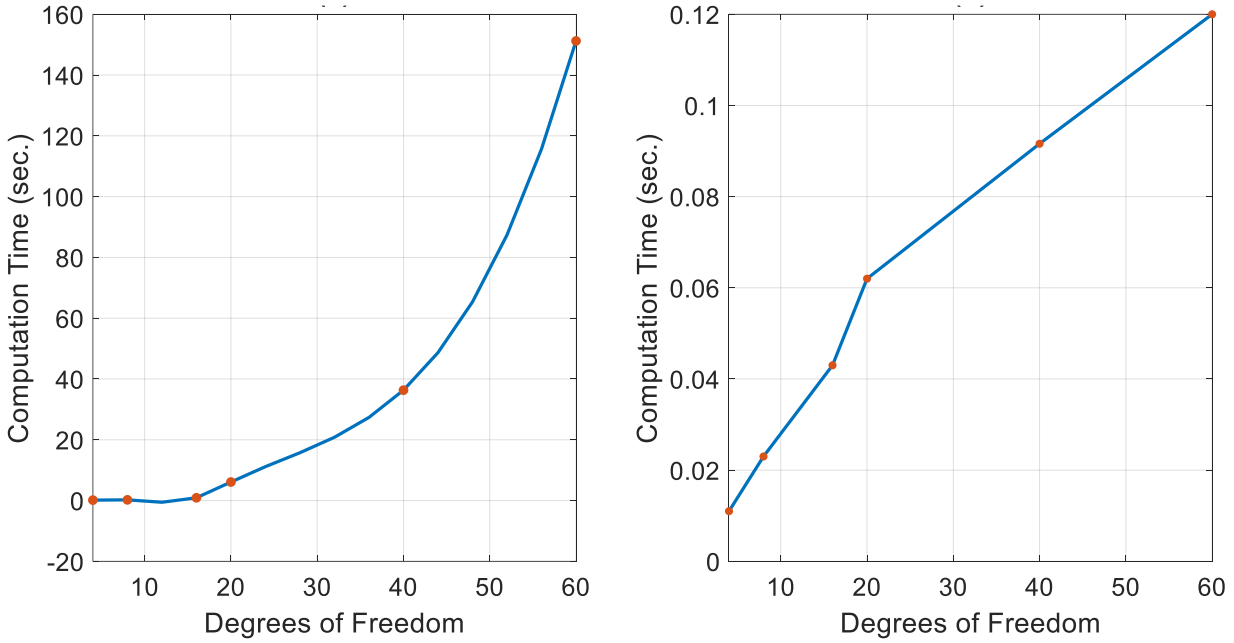

(a) (b)

Figure 10: Computation time with increase in DOF for a system of multiple-DOF second order differential equations using (a) the numerical method (ode45 solver in MATLAB), (b) the proposed analytical method.

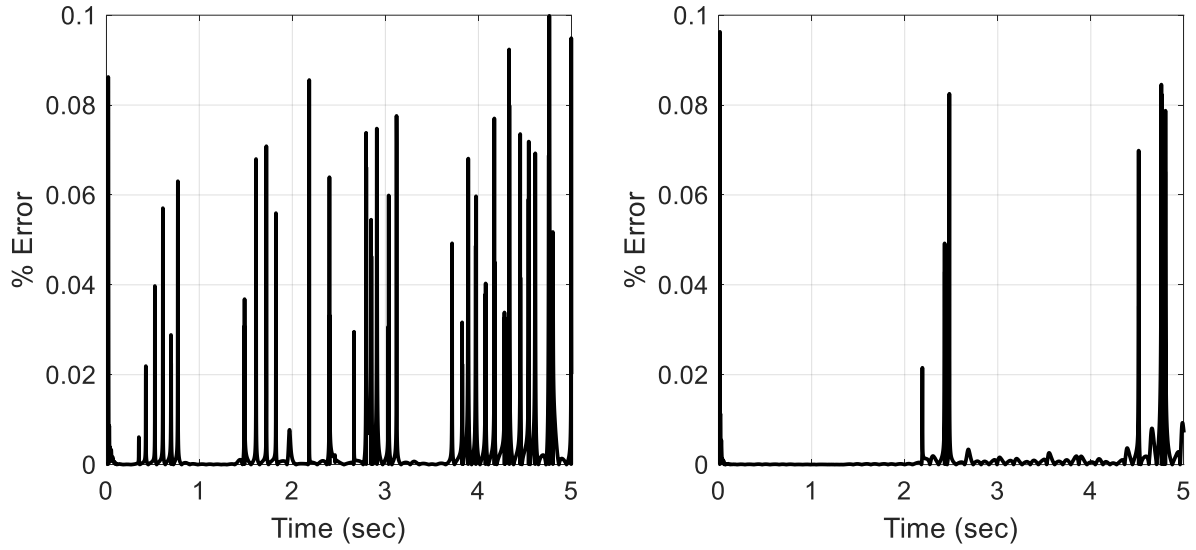

(a) (b)

Figure 11: Percentage error of displacements with time between the proposed analytical method and the numerical method (using ode45) in MATLAB® for the 20 DOF second order system of differential equations at a) the 4th degree of Freedom and b) the 18th degree of freedom

2.6.2. Free Vibration: Eigenfrequencies and Mode Shapes

Free vibration in a mechanical structure or system refers to the absence of external forces when the system is allowed to vibrate freely with some initial conditions. Free undamped vibrations are the simplest to analyze. The mathematical expression for free vibration of a multiple degrees of freedom (DOF) undamped system is given as,

$$\mathbf{M}\ddot{\mathbf{x}} + \mathbf{K}\mathbf{x} = \mathbf{0} \tag{24}$$

Usually, the response due to free vibrations of a system is harmonic in nature [71]. Therefore, we can assume a solution of equation (24) as,

$$\mathbf{x} = \mathbf{u}e^{j\omega_k t} \tag{25}$$

Substituting (25) in (24) gives,

$$\left[\mathbf{K} - \omega_k^2\mathbf{M}\right]\mathbf{u} = \mathbf{0} \tag{26}$$

For a non-trivial solution, the following must be true,

$$|\mathbf{K} - \omega_k^2\mathbf{M}| = \mathbf{0} \tag{27}$$

Equation (27) is the eigenvalue problem and can be solved for multiple-DOF systems using numerical solvers, for example, with the command *eig*(**K**,**M**) in MATLAB. For an n-DOF system, the numerical solvers like *eig* in MATLAB returns two matrices as shown below,

$$\mathbf{\Lambda} = \begin{bmatrix} \lambda_1 & & & \\ & \lambda_2 & & \\ & & \ddots & \\ & & & \lambda_n \end{bmatrix}, \quad \mathbf{V} = \begin{bmatrix} \mathbf{v}_1 \\ \mathbf{v}_2 \\ \vdots \\ \mathbf{v}_n \end{bmatrix}^T \tag{28}$$

Here, $\mathbf{\Lambda}$ is the diagonal matrix of the eigenvalues and **V** is the matrix containing all the eigenvectors $\mathbf{v}_k$ ($k=1,2,\ldots n$) associated with eigenvalues λ_k ($k=1,2,\ldots n$). The eigenvalues are related with the original variable ω_k in (27) as $\omega_k = \sqrt{\lambda_k}$ ($k=1,2,\ldots n$). Moreover, the eigenvector matrix **V** is equal to the matrix **u** ($=[\mathbf{u}_1 \quad \mathbf{u}_2 \quad \cdots \quad \mathbf{u}_n]$).

The eigenfrequencies, also known as natural frequencies, are the frequencies at which a system tends to vibrate without the application of any external force. From (27), ω_k ($k=1,2,\ldots n$) are the eigenfrequencies of the system. A mode shape of a mechanical system refers to a specific pattern of deflection or displacement that corresponds to a particular eigenvector or mode. It illustrates how different parts or DOF of the system move in relation to each other for that particular mode. From (26) & (28), the *nx1* vectors $\mathbf{u}_k = \mathbf{v}_k$ ($k=1,2,\ldots n$) represents the mode shapes for the respective modes ω_k ($k=1,2,\ldots n$).

To demonstrate the computation of the eigenfrequencies and mode shapes, we consider an example 2 DOF undamped system as shown in Figure 12. The system parameters are taken as $m_1 = 18$ *kg*, $m_2 = 2$ *kg*, $k_1 = 48$ *N/m*, and $k_2 = 6$ *N/m*. The global mass and stiffness matrices of the system in Figure 12 are as follows,

$$\mathbf{M} = \begin{bmatrix} m_1 & 0 \\ 0 & m_2 \end{bmatrix}, \quad \mathbf{K} = \begin{bmatrix} k_1 + k_2 & -k_2 \\ -k_2 & k_2 \end{bmatrix} \tag{29}$$

Using the global mass and stiffness matrices in (29), the governing differential equation of the example system for free vibration is expressed as in (24). We solve the eigenvalue problem in MATLAB using the *eig*(**K**,**M**), which returns the following eigenvalue and eigenvector matrices.

$$\mathbf{\Lambda} = \begin{bmatrix} 2 & 0 \\ 0 & 4 \end{bmatrix}, \quad \mathbf{V} = \begin{bmatrix} -0.1667 & -0.1667 \\ -0.5 & 0.5 \end{bmatrix} \tag{30}$$

Therefore, the example system in Figure 12 has two eigenfrequencies $\omega_1 = \sqrt{2}$ and $\omega_2 = 2$. The corresponding eigenvectors or mode shapes for each mode are $\mathbf{u}_1 = [-0.1667 \quad -0.5]^T$ and $\mathbf{u}_2 = [-0.1667 \quad 0.5]^T$. The mode shapes are plotted for each DOF and shown in Figure 13 to get

a relative displacement of each degrees of freedom for each mode. For discrete approximation of continuous structures, we compute the eigenvector matrix and for each mode, the corresponding eigenvector can be interpolated throughout the structure for visualization purpose.

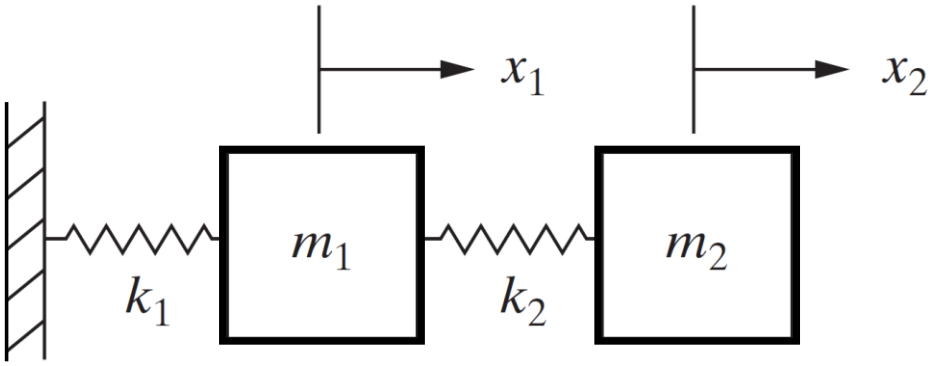

Figure 12: Example 2 DOF undamped system

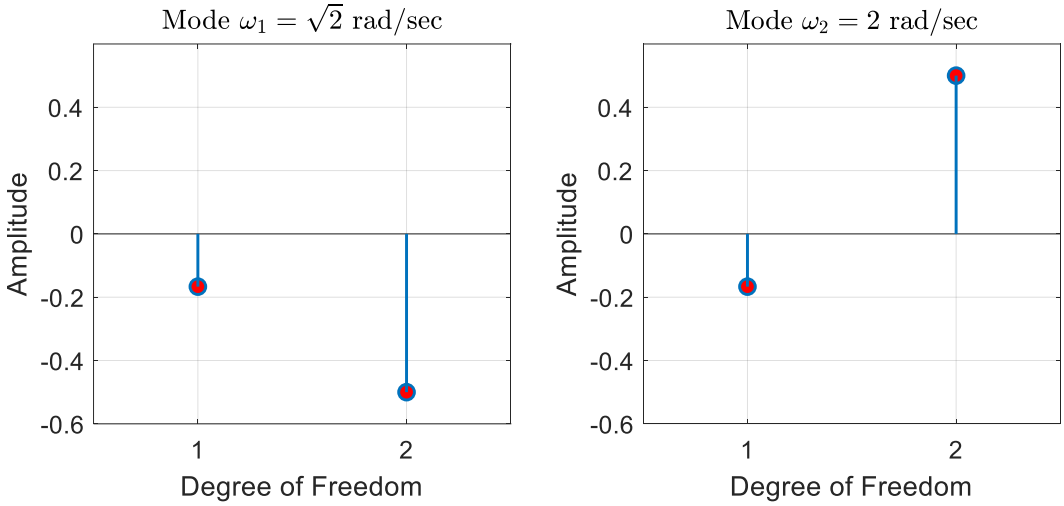

Figure 13: Mode shapes of the example system in Figure 12

We have demonstrated how eigenfrequencies and mode shapes can be computed for multiple DOF systems in this section. This will be utilized in the future chapters as a tool.